Intermolecular vibrations and fast relaxations in supercooled ionic liquids

JOURNAL OF CHEMICAL PHYSICS, v.134, n.24, 2011
http://producao.usp.br/handle/BDPI/16816

Intermolecular vibrations and fast relaxations in supercooled ionic liquids

Mauro C. C. Ribeiro

Citation: J. Chem. Phys. **134**, 244507 (2011); doi: 10.1063/1.3604533
View online: http://dx.doi.org/10.1063/1.3604533
View Table of Contents: http://jcp.aip.org/resource/1/JCPSA6/v134/i24
Published by the American Institute of Physics.

Intermolecular vibrations and fast relaxations in supercooled ionic liquids

Mauro C. C. Ribeiro[a)]
Laboratório de Espectroscopia Molecular, Instituto de Química, Universidade de São Paulo, CP 26077, CEP 05513-970, São Paulo, SP, Brazil

(Received 24 February 2011; accepted 7 June 2011; published online 28 June 2011)

Short-time dynamics of ionic liquids has been investigated by low-frequency Raman spectroscopy ($4 < \omega < 100$ cm^{-1}) within the supercooled liquid range. Raman spectra are reported for ionic liquids with the same anion, bis(trifluoromethylsulfonyl)imide, and different cations: 1-butyl-3-methylimidazolium, 1-hexyl-3-methylimidazolium, 1-butyl-1-methylpiperidinium, trimethylbutylammonium, and tributylmethylammonium. It is shown that low-frequency Raman spectroscopy provides similar results as optical Kerr effect (OKE) spectroscopy, which has been used to study intermolecular vibrations in ionic liquids. The comparison of ionic liquids containing aromatic and non-aromatic cations identifies the characteristic feature in Raman spectra usually assigned to librational motion of the imidazolium ring. The strength of the fast relaxations (quasi-elastic scattering, QES) and the intermolecular vibrational contribution (boson peak) of ionic liquids with non-aromatic cations are significantly lower than imidazolium ionic liquids. A correlation length assigned to the boson peak vibrations was estimated from the frequency of the maximum of the boson peak and experimental data of sound velocity. The correlation length related to the boson peak (~19 Å) does not change with the length of the alkyl chain in imidazolium cations, in contrast to the position of the first-sharp diffraction peak observed in neutron and X-ray scattering measurements of ionic liquids. The rate of change of the QES intensity in the supercooled liquid range is compared with data of excess entropy, free volume, and mean-squared displacement recently reported for ionic liquids. The temperature dependence of the QES intensity in ionic liquids illustrates relationships between short-time dynamics and long-time structural relaxation that have been proposed for glass-forming liquids. © *2011 American Institute of Physics*. [doi:10.1063/1.3604533]

I. INTRODUCTION

Technological applications of ionic liquids, i.e., room temperature molten salts, as new solvents, electrolytes, extraction media, etc. have demanded fundamental physicochemical characterization and extensive measurements of thermal properties and transport coefficients, such as diffusion coefficient, ionic conductivity, viscosity, and thermal conductivity.[1–6] A common finding resulting from the thermophysical studies is that many ionic liquids are easily supercooled upon reduction of temperature below the melting temperature T_m, and their glass transition temperature T_g is typically around 190 K.[7–9] Transport coefficients change with temperature in such a way that prompts the classification of ionic liquids as fragile glass-forming liquids.[10–12] Fragility of a supercooled liquid measures the departure from an strict linear behavior of the viscosity at temperature close to T_g in an Arrhenius plot, $\log(\eta)$ vs. $1/T$.[13,14]

Several spectroscopic techniques have been used to study ionic liquids aiming a microscopic understanding of macroscopic properties and eventual designing of new systems.[15,16] For instance, dielectric relaxation spectroscopy has been used to investigate ionic liquids dynamics in a broad frequency range,[17–19] and neutron scattering spectroscopy to unravel dynamics processes occurring within the nanosecond range.[11,20] Short-time intermolecular dynamics of ionic liquids has been investigated mainly by optical Kerr effect (OKE) spectroscopy[16,21–26] covering a frequency range similar to low-frequency Raman spectroscopy. Raman spectra of glass-forming liquids exhibit a quasi-elastic scattering (QES) centered at zero frequency with few wavenumbers of bandwidth due to fast (picosecond) relaxational motions.[27–34] In OKE spectroscopy, these relaxations take place in time domain slower than the intermolecular vibrations, but they are called fast relaxations in low-frequency Raman spectroscopy in comparison to long-time structural relaxation (the α relaxation) of supercooled liquids. The fast relaxations probed by low-frequency Raman spectroscopy at THz frequency range are sometimes called the fast β relaxation within the framework of the mode coupling theory, and should not be confused with the Johari-Goldstein relaxation (slow β relaxation) at frequencies about six orders of magnitude smaller.[34,35] The QES intensity, I_{QES}, decreases markedly when the temperature decreases, and a broad band due to intermolecular vibrational dynamics, the so-called boson peak, appears for the supercooled liquid close to T_g. Overall, as more fragile is the glass-forming liquid, smaller is the relative intensity of vibrational to relaxational contributions in low-frequency Raman spectra.[33,34] The parameter $R_1 = I_{\mathrm{min}}/I_{\mathrm{bp}}$, where I_{bp} is the boson peak intensity and I_{min} is the intensity at the minimum in frequencies below the boson peak, has been proposed in Ref. 33 in order to quantify the ratio between relaxational and vibrational contributions at T_g. Evaluation of R_1 might not be accurate for the fragile ionic liquids, so that rather than rely on

a)Electronic mail: mccribei@iq.usp.br.

R_1 for a single spectrum at T_g, we will discussed here instead the rate of change of I_{QES} with temperature.

Ionic liquids have been the subject of Raman spectroscopy measurements within the high frequency range in order to investigate ionic structures, conformations of side chains, hydrogen bonding between anion and cation, etc.[36–39] In contrast to previous works dealing with intramolecular vibrations, this work focuses on the intermolecular dynamics of ionic liquids at the low-frequency range of the Raman spectrum, $4 < \omega < 100$ cm^{-1}. The OKE spectroscopy has given important insights on intermolecular dynamics of ionic liquids, for instance, the librational motions (hindered rotations) of the aromatic ring in imidazolium and pyridinium ionic liquids.[16,21–26] In principle, OKE and Raman spectra give the same information because both techniques probe polarizability fluctuations. In OKE spectroscopy, the time domain data are Fourier transformed resulting in an intermolecular vibrational spectrum without long time relaxation.[21–26,40] In case of ionic liquids, much more attention has been given to these vibrational components revealed by OKE spectroscopy, but in the context of glass-forming liquids, the temperature dependence of fast relaxations observed as the QES intensity in Raman spectra is also an important issue.[27–34]

In this work, low-frequency Raman spectra are investigated for five different ionic liquids containing a common anion, bis(trifluoromethylsulfonyl)imide, [Tf_2N], and different cations, including aromatic, non-aromatic cyclic, and tetraalkylammonium cations. Figure 1 shows schematic structures and abbreviations of the species investigated in this work: [bmIm][Tf_2N], [hmIm][Tf_2N], [bmPip][Tf_2N], [bmmmN][Tf_2N], and [bbbmN][Tf_2N]. The systems have been chosen in order to unravel the effect on the Raman spectra of changing the length of the alkyl chain, replacing aromatic by an aliphatic ring, and also replacing the polar part of cations from a planar imidazolium ring to a more spherical moiety in tetraalkylammonium cations. On the other hand, while keeping the [Tf_2N] anion, we can compare Raman intensity of different systems in the low-frequency range after normalizing the spectra by the high frequency Raman bands of the anion, in the same way as one usually normalizes low-frequency Raman spectra of a given system at different temperatures.

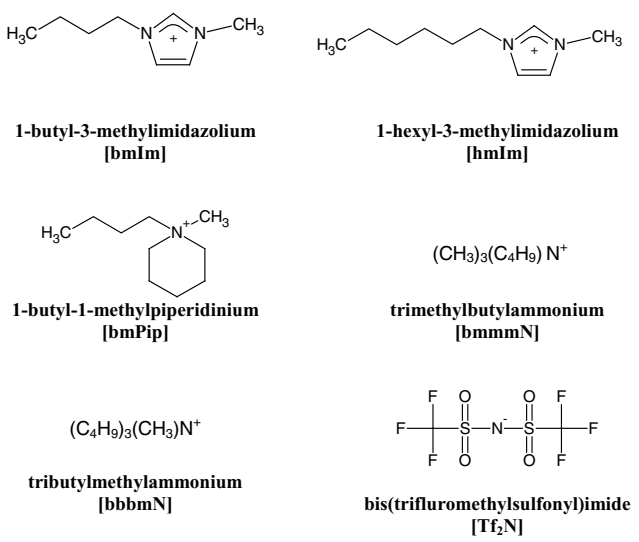

FIG. 1. Schematic structures and abbreviations of ionic liquids investigated in this work.

The aim of this work is twofold. Taking [bmIm][Tf_2N] as an example, we first shown in Sec. III A that low-frequency Raman spectroscopy provides the same information on intermolecular vibrations as previous OKE spectroscopy investigations of ionic liquids. This allows the discussion of some assignments already proposed in OKE measurements of ionic liquids. However, the main focus of the analysis of the intermolecular vibrations is its relationship to QES intensity in Raman spectra of glass-forming liquids. The second aim of this work relies on several correlations that have been proposed between short-time dynamics and fragility of glass-forming liquids.[41] This is discussed in Sec. III B, where the temperature dependence of fast relaxations given by the QES intensity is compared with quantities related to different theories for transport coefficients in supercooled liquids. The I_{QES} is compared with excess entropy involved in the Adam-Gibbs theory,[42] mean hole volume involved in free volume theories,[43,44] and also mean square displacement[45] recently available for some ionic liquids. In the particular case of [hmIm][Tf_2N], for which structural relaxation has been investigated within a wide temperature range, $185 < T < 430$ K,[11] it will be shown that the $I_{QES}(T)$ dependence unravels the characteristic temperatures T_o, T_g, and T_c, related to relaxation dynamics of glass-forming liquids.

II. EXPERIMENTAL

Raman spectra have been recorded in the Stokes side with a Jobin-Yvon T64000 triple monochromator spectrometer equipped with CCD. In order to record Raman spectra as close as 4.0 cm^{-1} from the exciting laser line, the Jobin-Yvon T64000 spectrometer was used in the subtractive configuration. The spectral resolution was 2.0 cm^{-1}. It has been found constant depolarization ratio in the low-frequency range, so that similar bandshapes are observed for polarized I_{VV}, depolarized I_{VH}, and also with no polarization selection. The ionic liquids were purchased from Iolitec, and dried under high vacuum (below 10^{-5} mbar) for more than 48 h. Karl-Fischer analysis indicated that water content in the ionic liquids is reduced below 30 ppm. The samples were dried inside the cryostat used to record Raman spectra at low temperatures, an Optistat^{DN} cryostat of Oxford Instruments. Raman spectra of some ionic liquids, in particular those which are pale yellow, might present a fluorescence background when excited with 514.5 nm, so that we used a 647.1 nm line of a Coherent Innova 90 Kr^+ laser.

III. RESULTS AND DISCUSSION

A. Intermolecular vibrations

Typical low-frequency Raman spectra of glass-forming liquids are illustrated with the ionic liquid [bmim][TF_2N] in Fig. 2. The QES intensity decreases at low temperatures in such a way that the vibrational contribution appears as

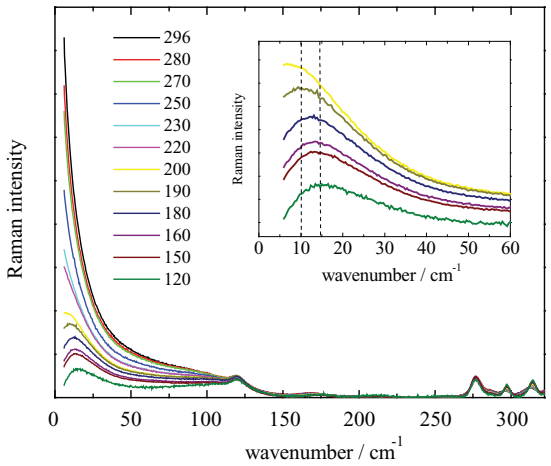

FIG. 2. Raman spectra of [bmIm][TF_2N] at temperatures indicated in the figure (T in Kelvin) normalized by the intensity of high frequency bands. The inset highlights the Raman spectra at low temperatures. The two vertical dashed lines indicate the position of the maximum at 190 and 120 K in order to help visualization of the shift of the boson peak with temperature.

a broad band with maximum at ~15 cm^{-1}, the so-called boson peak. Since the boson peak is usually more intense in strong than fragile glass-formers,[27–34] and typical ionic liquids are fragiles,[10–12] it is expected that the boson peak should be clearly seen in the raw Raman spectrum of [bmim][TF_2N], without reduction schemes discussed below that drops the QES intensity, only at temperatures close to its glass transition (T_g = 181.5 K).[46] In an investigation of 1-ethyl-3-methylimidazolium tosylate, [emIm][TSO], by OKE spectroscopy,[23] it has been observed the boson peak directly in the time domain data for this ionic liquid slightly above its T_g. In the time domain, the boson peak in [emIm][TSO] was manifest as an oscillatory component with period of ~2.0 ps.[23] Such oscillation period is consistent with the position of the boson peak found in the low-frequency Raman spectra for the ionic liquids investigated in this work. The inset of Fig. 2 highlights the low temperature spectra in order to show the upward frequency shift of the boson peak as temperature is reduced. This finding is a characteristic feature of the temperature dependence of the position of the boson peak,[34] which is usually associated with acoustic modes of wavelength compared to a correlation length ξ that will be discussed below. On the other hand, it is worth mentioning that recent measurements as a function of pressure indicated that modifications of elastic constants cannot account for the shift of the boson peak in SiO_2.[47] Unfortunately, high frequency elastic constants have not been measured for ionic liquids at deep supercooled liquid states close to T_g. Other intermolecular vibrations are seen in the low-frequency range, in particular the broad band with maximum at ~100 cm^{-1} which is assigned to librational motion of the imidazolium ring (see below). It should be noted that the band at 120 cm^{-1} is an intramolecular band of the [Tf_2N] anion, since it occurs in ionic liquids containing this anion.

Depolarized Raman and OKE spectra differ by a population factor,[48] so that the susceptibility representation, $\chi''(\omega) = I(\omega)/[n(\omega) + 1]$, where $I(\omega)$ is the experimental Raman spectrum, and $n(\omega) = [\exp(h\omega/kT) - 1]^{-1}$, should be comparable to the OKE spectrum. Low-frequency Raman spectra of glass-forming liquids are sometimes reported in the $\chi''(\omega)$ representation because of the relation between $I(\omega)$ and the vibrational density of states $\rho(\omega)$:[27–34,49,50]

$$I(\omega) = \frac{n(\omega)+1}{\omega} C(\omega)\rho(\omega), \quad (1)$$

where $C(\omega)$ is the light-vibration coupling. Another common representation is the reduced Raman intensity, $I_{red}(\omega) = I(\omega)/(\omega[n(\omega) + 1])$. Since the factor $[n(\omega) + 1]^{-1}$ depends linearly with ω at low-frequencies, $I_{red}(\omega)$ is similar to the experimental $I(\omega)$, whereas in the $\chi''(\omega)$ representation the position of the boson-peak is slightly shifted to higher frequencies.[50]

It will be first shown, using as example [bmIm][Tf_2N], that the low-frequency Raman spectra of ionic liquids are consistent with previous results obtained by OKE spectroscopy. The broad band observed in OKE spectra of ionic liquids within the $0 < \omega < 150$ cm^{-1} range has been fit with different functions previously used in several works on molecular liquids.[40] However, such broad spectral feature precludes to distinguish fit procedures on the basis of best agreement to experiment. Differences of experimental data between different authors are illustrated in Figs. 3(b)–3(d) by three fits proposed for the OKE spectrum of [bmim][TF_2N] at room temperature.[21,22,25] Figure 3(a) shows the Raman spectrum of [bmim][TF_2N] in the $\chi''(\omega)$ representation at room temperature, together with the fit by using three functions to reproduce the spectrum below 100 cm^{-1} (the intramolecular band of the [Tf_2N] anion is easily modelled by a Lorentzian band at 120 cm^{-1}, not shown in Fig. 3). The QES intensity in the Raman spectrum has been reproduced by a Lorentzian band centered at zero wavenumber with 5.0 cm^{-1} of bandwidth (thin black line in Fig. 3(a)). The vibrational component shown by a red line in Fig. 3(a) is a log-normal function:[51,52]

$$I_{bp}(\omega) = Ae^{-\frac{(\ln\omega - \ln\omega_{bp})^2}{\sigma^2}}, \quad (2)$$

where A is an arbitrary intensity factor, ω_{bp} = 16.7 cm^{-1} is the peak position, and σ = 1.22 cm^{-1} is related to the full width at half maximum as FWHM = $\omega_{bp}\{\exp[\sigma(\ln 2)^{1/2}] - \exp[-\sigma(\ln 2)^{1/2}]\}$, (FWHM = 40.1 cm^{-1} from the best fit shown in Fig. 3(a)). A log-normal function has been usually employed to model the boson peak in low-frequency Raman spectra of glass-forming liquids, and here we use it as a phenomenological function for fitting and comparing Raman and OKE spectra. The physical motivation of the log-normal function is to provide, as long as the velocity of sound propagation is available, the size distribution of clusters that would be present in the supercooled liquid and the glassy phase.[51] We will return below to a rough estimate of this correlation length since experimental values of sound velocity have been reported for some ionic liquids. Two other intermolecular vibrational modes shown in Fig. 3(a) by blue lines are Gaussian functions centered at 64 and 102 cm^{-1}.

OKE spectra of [bmim][TF_2N] have been fit with different number of bands and functional forms. In Fig. 3(b),[25] the thin black line is an Ohmic function:

$$I_O(\omega) = A\omega e^{-\frac{\omega}{\omega_o}}, \quad (3)$$

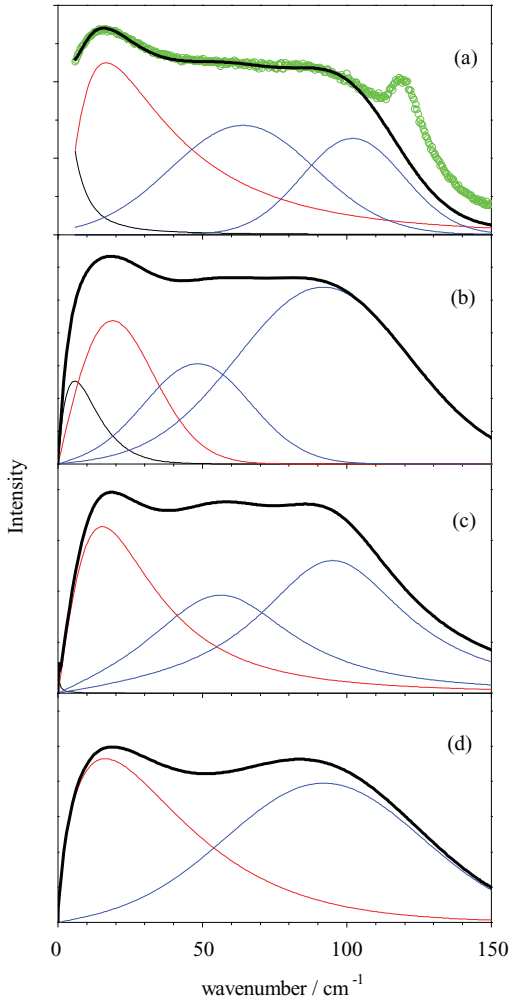

FIG. 3. (a) Raman spectrum of [bmIm][Tf_2N] at room temperature in the susceptibility representation (green symbols), total fit (black bold line), and individual components of the fit (black, red, and blue lines, as discussed in the text). Total fit of OKE spectra of [bmim][Tf_2N] (bold black line) and individual components: (b) Ref. 25; (c) Ref. 22; and (d) Ref. 21.

where A is an amplitude, and ω_o is the characteristic frequency. The red and blue lines in Fig. 3(b) are three antisymmetrized Gaussian functions:[25]

$$I_G(\omega) = A\left\{e^{-\frac{2(\omega-\omega_G)^2}{\sigma^2}} - e^{-\frac{2(\omega+\omega_G)^2}{\sigma^2}}\right\}, \quad (4)$$

where A is an amplitude factor, σ is the width, and ω_G is the center frequency (the best fit ω_G parameters provided in Table I of Ref. 25 are 9.4, 48.3, and 91.8 cm^{-1}). The first of these antisymmetrized Gaussian functions is shown in Fig. 3(b) by a red line in order to highlight its correspondence to the same component in 3(a), 3(c),[22] and 3(d).[21] In Fig. 3(c),[22] the OKE spectrum has been fitted by three damped harmonic oscillator (DHO) functions:

$$I_{\mathrm{DHO}}(\omega) = A\frac{\gamma\omega}{\left(\omega_o^2 - \omega^2\right)^2 + \gamma^2\omega^2}, \quad (5)$$

where A is an amplitude factor, γ is the damping rate, and ω_o is the frequency of the mode (the best fit ω_o parameters provided in Table I of Ref. 22 are 29.0, 64.0, and 100.0 cm^{-1}). The OKE spectrum of [bmim][TF_2N] reported in Ref. 21 was fit by only two bands as shown in Fig. 3(d), where the component given by a red line is a Bucaro-Litovitz (BL) function:

$$I_{\mathrm{BL}}(\omega) = A\omega^a e^{-\frac{\omega}{\omega_o}}, \quad (6)$$

where A is an amplitude factor, the parameter $a = 0.71$, and $\omega_o = 23.0\ cm^{-1}$. The BL function has been proposed on the basis of a binary collision model in order to account for low-frequency spectra of atomic and molecular liquids.[53] The BL function has been used simply as an empirical function to fit the low frequency component of OKE spectra of ionic liquids, since the assumption of single event of a binary collision is not reasonable in light of local structures of closed packing of neighbouring anions and cations in ionic liquids. The broad component shown as a blue line in Fig. 3(d) is an antisymmetrized Gaussian function, Eq. (4), centered at $\omega_G = 92.0\ cm^{-1}$.[21]

The comparisons in Fig. 3 indicate that low-frequency Raman spectroscopy provides the same information on intermolecular dynamics as several investigations of ionic liquids by OKE spectroscopy. Since extensive comparisons of OKE spectra for many ionic liquids have been already reported,[11,21–26] we discuss here only some controversies by using the low-frequency Raman spectra of the ionic liquids investigated in this work. The broad band close to 100 cm^{-1} in OKE spectra of imidazolium and pyridinium ionic liquids has been assigned to librational motion of the aromatic ring of cations.[21–26] Strong support for such assignment is given in Fig. 4, which compares low-frequency Raman spectra of imidazolium, piperidinium, and tetralkylammonium ionic liquids in the $\chi''(\omega)$ representation. It is clear that the band close to 100 cm^{-1} assigned to librational motion of the imidazolium ring is missing in the non-aromatic ionic liquids. The comparison between aromatic and non-aromatic ionic liquids does not support the interpretation proposed in Ref. 22, where the three bands observed in OKE spectra (see Fig. 3(c)) have been assigned to three different librational motions of the imidazolium ring. Figure 4 also indicates that a more

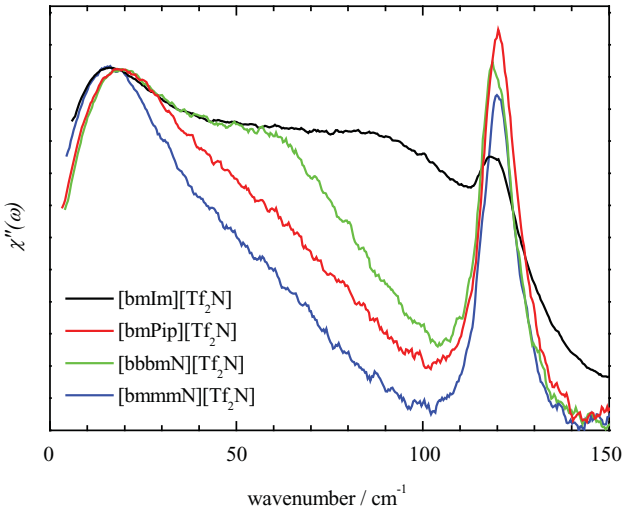

FIG. 4. Raman spectra in the susceptibility representation of [bmIm][Tf_2N], [bmPip][Tf_2N], [bbbmN][Tf_2N], and [bmmmN][Tf_2N] at room temperature. For comparison purposes, spectra have been normalized by the intensity of the lowest frequency band.

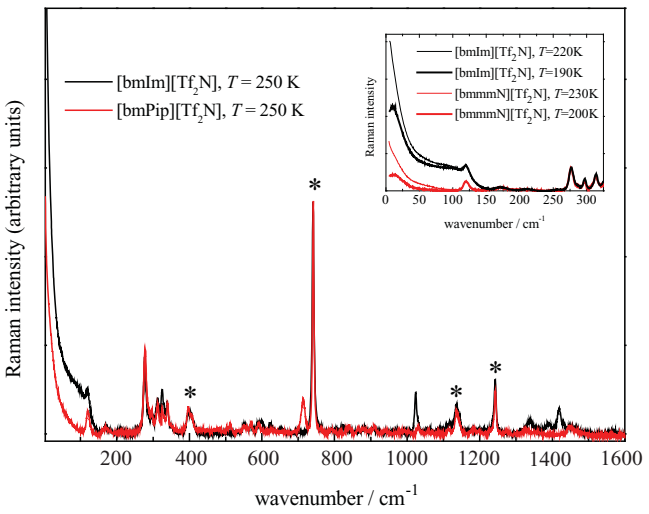

FIG. 5. Raman spectra of [bmIm][Tf_2N] (black) and [bmPip][Tf_2N] (red) at 250 K. The asterisks mark some of the [Tf_2N] bands used for intensity normalization. Inset shows the low-frequency range of normalized Raman spectra of [bmIm][Tf_2N] (black) and [bmmmN][Tf_2N] (red) at two different temperatures.

appropriate fit to low-frequency vibrational spectra of ionic liquids needs the component at ~65 cm^{-1} as in Figs. 3(a)–3(c), in contrast to the two components fit of Ref. 1 shown in Fig. 3(d). Since the Raman band at 100 cm^{-1} is assigned to libration of aromatic rings, whereas the 65 cm^{-1} band remains in all of the investigated ionic liquids, and also in others imidazolium ionic liquids with different anions,[32] it could be assigned to rattling motions, i.e., oscillatory hindered translations of a central ion inside the cage made by the neighbouring ions.

In the context of low-frequency Raman spectra of glass-forming liquids, an interesting analysis is the relationship between the lowest frequency vibrational component and the QES intensity. The investigation of ionic liquids with the same [Tf_2N] anion allows for comparisons of low-frequency Raman intensities between different systems. Thus, rather than the arbitrary normalization used in Fig. 4, some of the anion normal modes at high frequencies can be used to normalize the spectra in the same way as one usually normalizes low-frequency Raman spectra of a given system at different temperatures (see Fig. 2). Figure 5 compares Raman spectra of [bmIm][[Tf_2N] and [bmPip][[Tf_2N] at the same temperature, where some of the [Tf_2N] bands at wavenumbers higher than 400 cm^{-1} are indicated. The assignment of [Tf_2N] normal modes is easily done when one compares Raman spectra of ionic liquids containing [Tf_2N] vs. any halide anion, while keeping cation the same. Several bands due to the [Tf_2N] anion are seen around 300 cm^{-1}, but these normal modes might have significant contribution of conformational motions so that their intensities might be more dependent on temperature and the actual system. Further comparisons of low-frequency intensities are illustrated in the inset of Fig. 5 for [bmIm][[Tf_2N] and [bmmmN][[Tf_2N] close to the corresponding T_g, respectively, 181.5 and 195.0 K.[46,54]

It is clear from Fig. 5 that the Raman intensity in the low-frequency range is significantly higher for imidazolium ionic liquids because of the more polarizable moiety of the aromatic ring. Interestingly, within the range comprising the QES intensity and the maximum of the boson peak, say wavenumber smaller than 20 cm^{-1}, the ratio of the spectra of [bmIm][[Tf_2N] and [bmPip][[Tf_2N] is essentially constant at a given temperature, i.e., the very low-frequency range of the spectra of the investigated ionic liquids exhibit the same bandshape. In other words, independent of the relative intensities of relaxations and vibrations, both the contributions to the low-frequency Raman spectrum are simultaneously smaller in non-aromatic than aromatic ionic liquids. It has been proposed that the fast relaxation and the boson peak are correlated.[34] An important support for the correlation between the dynamics involved in the fast relaxation and the boson peak is that the depolarization ratio is the same for both contributions in Raman spectra of glass-forming liquids.[34] Frequency independent depolarization ratio has been also observed in this work and in previous investigations of ionic liquids.[30–32] Recently, the relationship between fast relaxation and boson peak has been reinforced by an investigation of Raman spectra as a function of pressure for several molecular and polymeric glass-former.[55] It has been found a linear correlation between the QES and the boson peak intensities for a given system as a function of pressure. Therefore, the finding shown in Fig. 5, i.e., both the QES and the boson peak intensity changing by the same amount in ionic liquids of similar fragilities, adds another piece of evidence for the interrelation between relaxational and vibrational contributions in low-frequency Raman spectra of supercooled liquids. Such correlation strengths the proposition of an indirect mechanism for the QES contribution,[56] for instance, as in the coupling model, in which the QES intensity increases with temperature due to damping of the boson peak vibrations.[34,55,57–59] Rather than a superposition model of two independent functions for QES and boson peak, the Raman spectrum is calculated in the coupling model by averaging a purely vibrational contribution, usually assumed as the Raman spectrum recorded at very low temperature, with a function giving the relaxations from all of the processes damping the vibrations. Both the superposition and the coupling models can give good fit to experimental spectra, for instance, see the studies of the glass-former $GeSBr_2$ (Ref. 60) and the ionic liquid [bmIm][PF_6].[31] Therefore, the coupling model is favored on the basis of arguments as mentioned above, but not just from better agreement to experiment.

The microscopic nature of the boson peak is a widely debated issue in the context of glass-forming liquids dynamics (see Ref. 55 and references therein). A length scale of domains with diameter 2ξ is usually assigned to the boson peak by the relation:

$$\xi = \frac{v_s}{(2\omega_{bp})}, \tag{7}$$

where ω_{bp} is the maximum of the boson peak and v_s is the sound velocity.[61,62] In this model, the size of these domains determines the limiting mean-free path that is responsible for phonon localization, and these localized motions result in an enhancement of the vibrational density of states [$\rho(\omega)$ in Eq. (1)]. It turns out that typical correlation length ξ is of the

order of 10–20 Å. Low-frequency Raman spectra of ionic liquids give similar magnitude of ξ. For instance, in the Raman spectrum of [bmIm][Tf_2N] close to the glass transition temperature, it is found $\omega_{bp} \sim 13\ cm^{-1}$. In case of [bmIm][$Tf_2N$], $v_s \sim 1230\ m\ s^{-1}$ at room temperature,[63–65] and a linear dependence has been measured within the 293–323 K range.[64] By using the temperature dependence in this restricted range, a rough estimate gives $v_s \sim 1500\ m\ s^{-1}$ close to T_g. Therefore, one obtains the length scale $\xi \sim 19$ Å related to the boson peak vibrations in [bmIm][Tf_2N].

It is interesting to compare the length ξ with the characteristic size of heterogeneities that has been obtained from the wave-vector of the first-sharp diffraction peak, k_{FSDP}, observed in neutron or X-ray spectra,[26,66–69] and also molecular dynamics (MD) simulations,[69–73] of ionic liquids. In the sequence of [emIm], [bmIm], and [hmIm] ionic liquids, k_{FSDP} shifts in such a way that the corresponding size of heterogeneities increases, 7, 11, and 15 Å, respectively.[26] In contrast, FSDP has been not observed in a recent x-ray scattering investigation of [bbbm][Tf_2N].[69] The FSDP in the static structure factor, $S(k)$, indicates that an intermediate-range order (IRO) develops in the liquid, but the nature of such IRO in glass-forming liquids is another lively debated issue because different explanations have been proposed. In SiO_2, the network of connected SiO_4^{2-} tetrahedral produces the correlations of the IRO.[74] In *m*-toluidine, IRO is due to clusters in a network of hydrogen-bonded molecules.[75] In concentrated aqueous solution of salts of di- or trivalent cations, X-ray diffraction data have been reproduced with a model of a hypothetical cubic arrangement of M^{2+} or M^{3+} cations that are positioned in relatively long distance between each other in order to minimize the strong coulombic repulsions.[76,77] It has been also suggested that IRO may arise from correlation of voids or layers in the bulk of a supercooled liquid.[78,79] In case of ionic liquids, k_{FSDP} shifts sequentially to lower values with increasing length of the alkyl chain in the cations.[26,66–68] MD simulations suggested that ionic liquids are structurally heterogeneous, in such a way that polar regions made of anions and the imidazolium ring of cations coexist with non-polar regions made of the side chains of cations.[70–73] On the other hand, the FSDP in ionic liquids has been recently assigned to correlation of the second shell of cations, with no need of a picture of nanoscale polar/non-polar heterogeneity.[68] However, it is worth stressing that the physical picture of structural heterogeneity in ionic liquids has been proposed by MD simulation not only on the basis of the occurrence of a FSDP in the calculated $S(k)$ but also on the basis of anions depletion in regions occupied by the alkyl chains.[70–73]

Several inorganic glass-formers present correlation between the characteristic length ξ obtained from the boson peak and from the FSDP.[61,62] This correlation between ξ^{-1} and k_{FSDP} has been explained for SiO_2 on the basis that the length ξ is ~3–4 times the cation – cation distance d, where d determines the position of the FSDP by $k_{FSDP} = 3\pi/2d$.[62] However, rather than compare very different systems, a systematic investigation of the glass-former B_2O_3 with different modifiers demonstrated failure of the linear relationship between ξ^{-1} and k_{FSDP}.[80] The modifiers were added in B_2O_3 in order to change the IRO but not the short-range correlation. A similar situation occurs if one compares 1-alkyl-3-methylimidazolium ionic liquids of alkyl chains of different lengths, while keeping the same anion: the nearest neighbour structure of anions around the imidazolium ring is almost not modified within polar regions, whereas the FSDP shifts to lower wave-vector for cations with longer carbon chain.[26,66–68] In this work, we have found no change of ω_{bp} in the Raman spectra of [bmIm][Tf_2N] and [hmIm][Tf_2N], and also in the 1-ethyl-3-methylimidazolium derivative, [emIm][Tf_2N], considered in a previous work.[32] The unchanged value of ω_{bp} in Eq. (7), together with the finding that the sound velocity of ionic liquids does not change as the length of the alkyl side chain increases while keeping the anion,[63–65] imply the same ξ from [emIm] to [hmIm] ionic liquids. Thus, failure of the linear relationship between ξ^{-1} and k_{FSDP} is evident because of the downshift of k_{FSDP} in ionic liquids with increasing length of the alkyl chain. Even though a scale length ξ might be assigned to the boson peak vibrations, effects such as the type of the low-frequency vibrational modes have been considered as the origin of the failure of a linear correlation between ξ^{-1} and k_{FSDP}.[80] Thus, the strength of bonding forces within a given domain, i.e., the magnitude of interactions between neighbouring anions and cations in ionic liquids, might be relevant to the actual value of ω_{bp}. In fact, both the ω_{bp} and the v_s are more dependent on the anion, while keeping the same cation. For instance, v_s for [bmim][Tf_2N] and [bmim][BF_4] are, respectively, 1230 (Refs. 63–65) and 1565 $m\ s^{-1}$.[63,81] In a previous Raman investigation of imidazolium ionic liquids with different anions,[32] it has been found that ω_{bp} in these systems change by the same amount, respectively, 13 and 17 cm^{-1}.

B. Fast relaxations

Fragility of glass-forming liquids, $m = d\ln[\eta(T)]/d(T_g/T)$ at $T \to T_g$, where η is the viscosity, has been correlated to different indicators of fast dynamics. For instance, it has been related to the non-ergodic factor calculated from the plateu regime of the intermediate scattering function obtained by inelastic X-ray scattering spectroscopy,[82,83] to the amplitude of mean-square displacement obtained from neutron scattering spectroscopy,[45,84] and to elastic properties such as the infinity frequency limit of the shear modulus.[41,85] In low-frequency Raman spectroscopy, it is known that the temperature dependence of the QES intensity, I_{QES}, in the supercooled liquid range is steeper than below T_g.[27–34,57–60] The change of slope of the $I_{QES}(T)$ curve at T_g is at first sight a remarkable finding, since QES is related to processes taking place at picosecond time scale while the glass transition is due to the structural α-relaxation time, τ_α, reaching 10^2–10^3 s. In fact, the relationship between I_{QES} and α-relaxation is another example of these correlations between fast and slow dynamics of glass-forming liquids.

The temperature dependence of I_{QES} can be obtained from fit of experimental data by using either the superposition or the coupling models for the relaxational and vibrational contributions of low-frequency Raman spectra.[57–60] It has been already shown that both the models give good fit to

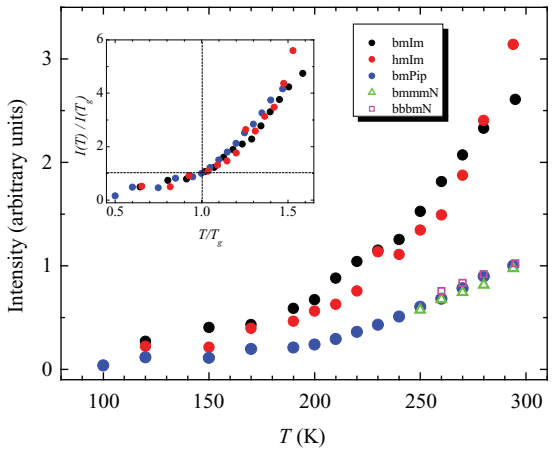

FIG. 6. Temperature dependence of I_{QES} of ionic liquids based on the [Tf_2N] anion and different cations: [bmIm], [hmIm], [bmPip], [bmmmN], and [bbbmN], as indicated in the figure. Inset shows I_{QES} for [bmIm][Tf_2N], [hmIm][Tf_2N], and [bmPip][Tf_2N], normalized by the corresponding value at the glass transition temperature, respectively, 181.5 (Ref. 46), 183 (Refs. 11, 86, and 87), and 200 K (Ref. 88). The symbols are of the size of estimated error bars.

Raman spectra of the ionic liquid [bmIm][PF_6],[31] but these models need assumptions concerning the functions to be used in fits. Thus, we follow here instead a less model dependent procedure, and we considered I_{QES} as the integral up to the boson peak, say $4 < \omega < 20$ cm^{-1}, of the experimental spectrum normalized by intensity of high frequency bands. Figure 6 shows $I_{QES}(T)$ for the ionic liquids investigated in this work. It has been observed partial crystallization of the tetralkylammonium ionic liquids during cooling, so that I_{QES} for [bmmmN][Tf_2N] and [bbbmN][Tf_2N] are shown in Fig. 6 within a narrower temperature range. The I_{QES} for the imidazolium ionic liquids are clearly larger than piperidinium and tetralkylammonium ionic liquids, but the inset of Fig. 6 shows that the intensities normalized by the values at the corresponding T_g follow essentially the same behavior. In a previous work on imidazolium ionic liquids with different anions, the rate dI_{QES}/dT in the supercooled liquid range has been related to fragility.[32] It has been found that dI_{QES}/dT depends more on changing the anion than changing of length of the alkyl chain in imidazolium cations. Thus, the main conclusion drawn from Fig. 6 is that the finding of Ref. 32 is also valid for non-aromatic ionic liquids with the same [Tf_2N] anion.

The non-Arrhenius behavior of transport coefficients in fragile supercooled liquids indicates that the effective activation energy, E_a, is itself temperature dependent, $\eta \propto \exp[E_a(T)/RT]$. Experimental data for ionic liquids have been fit with one of the most common empirical formula, i.e., the Vogel-Fulcher-Tamman (VFT) equation:[13,14]

$$\eta = Ae^{\frac{B}{T-T_o}}, \tag{8}$$

where A, B, and T_o are adjustable parameters. Several theories are able to reproduce the behavior like the VFT equation. In the Adam-Gibbs (AG) theory,[42] the focuses relies on the temperature dependence of the configurational entropy, S_c:

$$\eta \propto \exp\left(\frac{C}{TS_c}\right), \tag{9}$$

where C is a constant. The AG theory is usually compared to experiment by replacing S_c by the excess entropy, S_{exc}, which is the difference between liquid and crystal entropies, even though S_c and S_{exc} are not the same quantity because the vibrational contribution to the entropy of the amorphous phase is not the same as the crystalline phase.[89–92] In free-volume theories,[43,44] the arrest of structural relaxation is due to reduction of free volume, V_f, available for particle displacement:

$$\eta \propto \exp\left(\frac{C}{V_f}\right), \tag{10}$$

where C is a constant. Experimental data of V_f are usually obtained from positron annihilation lifetime spectroscopy (PALS).[93] Viscosity has been also related to the Debye-Waller factor,[45,84] i.e., the amplitude of mean square displacement, $\langle u^2 \rangle$, of rattling motions of particles inside the cage made by the neighbours:

$$\eta \propto \exp\left(\frac{C}{\langle u^2 \rangle}\right), \tag{11}$$

where C is a constant. There is a steep increase of $\langle u^2 \rangle$ with increasing temperature around T_g, analogous to the Lindemann criterion for melting of crystals when $\langle u^2 \rangle$ exceeds a critical value.[45,84]

The $I_{QES}(T)$ curve obtained by low-frequency Raman spectroscopy is similar to the relevant properties in these theories. The top panel in Fig. 7 shows the [bmPip][Tf_2N] results for which linear behavior of $I_{QES}(T)$ is seen above and below T_g, with a crossover that essentially coincides with the experimental T_g.[88] By extrapolating the linear fit of the supercooled liquid range down to the glassy state, the estimate $T_o \sim 0.89T_g$ is typical of glass-forming liquids. Table I gives T_o values estimated by extrapolating the $I_{QES}(T)$ curves for the ionic liquids investigated in this work. Unfortunately, most of experimental data of viscosity of ionic liquids have been reported in a rather limited temperature range, mainly above room temperature. Once the VFT equation is fit to a limited temperature range, the parameters A, B, and T_o in Eq. (8) might be not accurate. For instance, the parameter T_o reported for [bmIm][Tf_2N] is too close to the corresponding T_g,[95] and most probably is an artifact resulting from VFT fit to high temperature viscosity. Interestingly, a second change of slope can be discerned within the supercooled range in the $I_{QES}(T)$ curves shown in Fig. 7 for [bmIm][Tf_2N] and [hmIm][Tf_2N]. In the following, the results for [hmIm][Tf_2N] will be discussed in more detail because a more complete picture of relaxation has been recently provided for this system along the whole range of the supercooled liquid by combining data of transport coefficients obtained by different techniques.[11]

Figure 8 compares $I_{QES}(T)$ of [hmIm][Tf_2N] (black circles) with some properties available for ionic liquids, all results normalized by the corresponding value at T_g. Data of excess entropy TS_{exc} for [hmIm][Tf_2N] are shown by the red line (see Fig. 5 in Ref. 87). We are not aware of experimental data of V_f for [hmIm][Tf_2N], but only to a very related

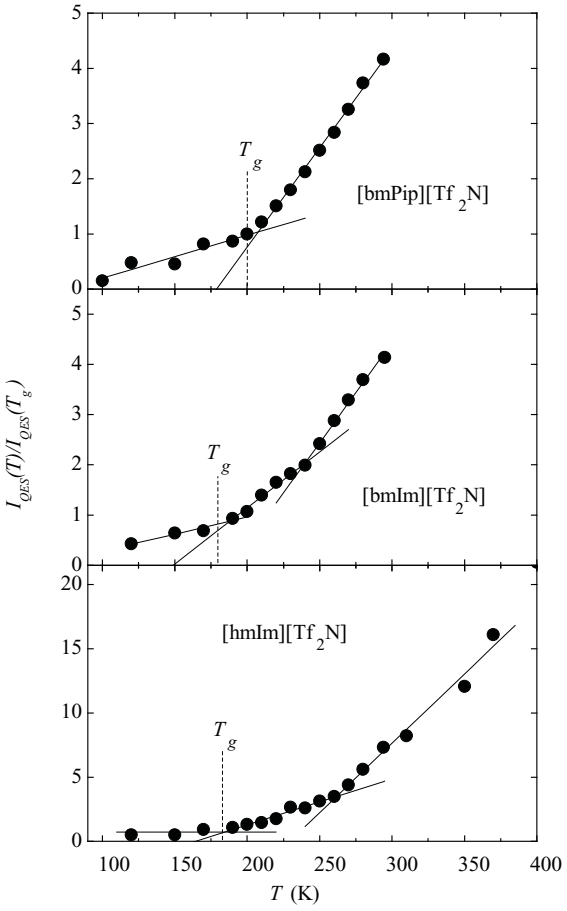

FIG. 7. Temperature dependence of I_{QES} of [bmPip][Tf_2N], [bmIm][Tf_2N], and [hmIm][Tf_2N]. Full lines are linear fits to glassy and supercooled liquid ranges. Vertical dashed lines indicate the experimental T_g given in Table I. The symbols are of the size of estimated error bars.

system containing the 1-propyl-3-methylimidazolium cation, [pmIm][Tf_2N] (green line in Fig. 8).[96] It is also shown by white triangles the mean square displacement $\langle u^2 \rangle$ obtained by neutron scattering measurements of the ionic liquid [bmIm]Cl (see Fig. 9 in Ref. 97). The similar temperature dependence of I_{QES} and the properties shown in Fig. 8 is understood on the basis of models for low-frequency Raman

TABLE I. Calorimetric glass-transition temperature, T_g, and characteristic temperatures, T_o and T_c, estimated in this work from the low-frequency Raman spectra of ionic liquids. Literature data of T_o obtained from the temperature dependence of viscosity are given in parenthesis.

	T_g (K)	T_o (K)	T_c (K)
[bmIm][Tf_2N]	181.5[a]	149 (180)[f]	236
[hmIm][Tf_2N]	183[b]	164 (155.2)[b]	262
[bmPip][Tf_2N]	200[c]	179	...
[bmmmN][Tf_2N]	195[d]	184 (186)[d]	...
[bbbmN][Tf_2N]	205[e]	162 (164.4)[e]	...

[a]Ref. 46.
[b]Refs. 11, 86, and 87.
[c]Ref. 88.
[d]Ref. 54.
[e]Ref. 94.
[f]Ref. 95.

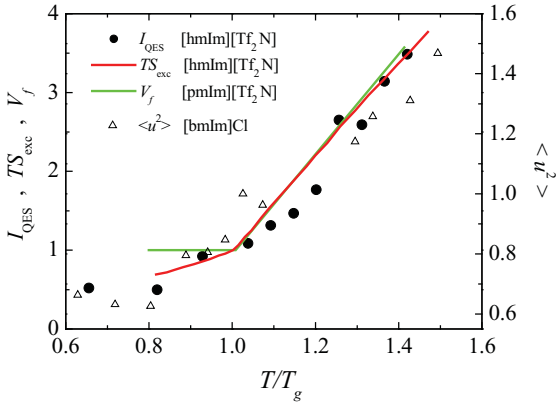

FIG. 8. Temperature dependence of QES intensity of [hmIm][Tf_2N] (black circles), excess entropy of [hmIm][Tf_2N] (red line) (Ref. 87), free volume of [pmIm][Tf_2N] (green line) (Ref. 96), and mean square displacement of [bmIm]Cl (triangles, scale at right) (Ref. 97). Data are presented normalized by the corresponding value at the glass transition temperature: T_g([hmIm][Tf_2N]) = 183 K (Refs. 11, 86, and 87), T_g([pmIm][Tf_2N]) = 183 K (Ref. 96), T_g([bmIm]Cl) = 225 K (Ref. 97). The black circles are of the size of estimated error bars.

spectra of glass-forming liquids.[57–59,98–100] In the coupling model,[57–59] the pronounced rise of I_{QES} above T_g is due to the increase of the coupling parameter, $\delta^2(T)$, between fast relaxations and the boson peak vibrations. The parameter $\delta^2(T)$ is the fraction of the relaxational to the vibrational plus relaxational contributions, so that $\delta^2(T)$ can be used as a measurement of $I_{QES}(T)$. It has been further assumed that the relaxations that promoted damping of the boson peak are due to free volume, so that a relationship between $\delta^2(T)$ and V_f has been proposed.[58,59] The data of $\langle u^2 \rangle$ for [bmIm]Cl are shown in Fig. 8 in a different scale. The relatively smaller slope $d\langle u^2 \rangle/dT$ should not be assigned to the different anion, instead the short-time scale of 1.0 ps concerned in the measurements in Ref. 97 is the origin of an apparent small increase of $\langle u^2 \rangle$ for [bmim]Cl. It has been suggested that $\langle u^2 \rangle$ should be evaluated in a time window of ~4.0 ns,[101] i.e., $\langle u^2 \rangle$ not purely vibrational but including relaxation, in order to reproduce the temperature dependence of the effective activation energy. In contrast, it has been also proposed that the time scale for $\langle u^2 \rangle$ should be smaller than structural relaxation, but beyond the very short-time range of the ballistic regime.[45] Most probably, the time window of 1.0 ps of the $\langle u^2 \rangle$ measurements in Ref. 97 is too short for scaling of structural relaxation in [bmim]Cl. The relationship between I_{QES} and $\langle u^2 \rangle$ is understood on the basis of a model in which relaxational like motion results from mixing of vibrational modes comprising the inhomogeneous distribution of the boson peak.[98–100] Thus, the glass to liquid transformation means vibrational to relaxational transformation of quasi-localized modes driven by the amplitude of structural fluctuations responsible for mixing of modes of the boson peak.

In line with a previous investigation of the ionic liquid [bmIm][PF_6],[31] a further relationship, that is between I_{QES} and S_{exc}, is suggested in Fig. 8 for [hmIM][Tf_2N]. The VFT fit to experimental data of structural relaxation of [hmIm][TF_2N] within the wide temperature range $185 < T < 430$ K provided best fit parameters $B = 890$ K and $T_o = 155.2$ K.[11]

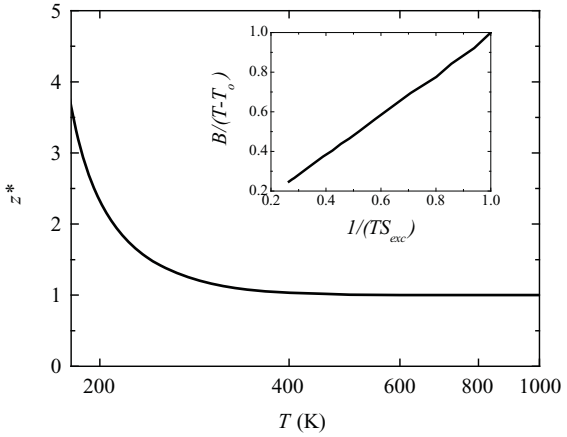

FIG. 9. The size of cooperatively rearranging regions calculated from the experimental S_{exc} of [hmIm][Tf_2N] after extrapolating S_{exc} of Ref. 87 to the high temperature limit. The inset shows the linear relationship between the experimental relaxation time of [hmIm][Tf_2N] given by $\ln\tau_\alpha \propto B(T-T_o)^{-1}$, Eq. (8), with the VFT parameters of Ref. 11 (B = 890 K, T_o = 155.2 K), and the AG theory, $\ln\tau_\alpha \propto (TS_c)^{-1}$, Eq. (9), with S_c replaced by S_{exc} of Ref. 87. The temperature range in the inset corresponds to the supercooled liquid range 183 < T < 270 K, and data in both the axes are normalized by the values at T_g.

Interestingly, T_o obtained from dynamics measurements agree with the extrapolated temperature at which S_{exc} of [hmIm][TF_2N] goes to zero, T_K = 154 K (see Fig. 5 in Ref. 87), i.e., the so-called Kauzmann temperature.[102] The finding $T_o \approx T_K$ gives support for analysing the structural relaxation on the basis of the AG theory.[89–91] Thus, a correlation plot between $B(T - T_o)^{-1}$ and $(TS_{\text{exc}})^{-1}$, Eqs. (8) and (9), holds within the supercooled liquid range of [hmIm][TF_2N], as shown in the inset of Fig. 9. In the AG theory,[42] the effective activation energy $E_a(T)$ increases from the high temperature limit, $\Delta\mu$, because of a growing size, $z^*(T)$, of cooperatively rearranging regions (CRR), $E_a(T) = \Delta\mu\ .z^*(T)$. The size $z^*(T)$ increases when temperature decreases because of its inverse dependence with the configurational entropy, $z^*(T) = S_c^*/S_c(T)$, where S_c^* is the high temperature limit of the configurational entropy. Thus, the temperature dependence of z^* is given by $1/S_c(T)$, with the asymptotic limit $z^* \to 1$ when $T \to \infty$. Figure 9 shows the calculated $z^*(T)$, where we considered $S_{\text{exc}} \propto S_c$, and extrapolated the $S_{\text{exc}}(T)$ data of [hmIm][TF_2N] of Ref. 87 to high temperatures. At the glass-transition temperature, one sees in Fig. 9 that $z^*(T_g)$ is around 3.5–4.0, which is a typical value found for many glass-formers, including a previous investigation of the ionic liquid [bmIm][PF_6].[31] This finding means that the average size of a CRR at T_g is 3.5–4.0 bigger than z^* at very high temperature. If one assumes that at least one pair of neighbouring ions must be involved in a relaxation event at very high temperature, and the distance between center of mass of anion and cation is 5.0 Å as calculated by MD simulations of [hmIm][TF_2N],[103] the size $z^*(T_g)$ corresponds to 17.5–20.0 Å. Therefore, the size $z^*(T_g)$ estimated from the AG theory is similar to the correlation length $\xi \sim$ 19.0 Å estimated in Sec. III A from the boson peak vibrations. In fact, this finding is in line with the proposition that the same structural skeleton is responsible for both the boson peak vibrations and the fast relaxations in low-frequency Raman spectra of glass-forming liquids.[98–100]

Even though the data of TS_{exc} and V_f in Fig. 8 do not correspond exactly to the same system, respectively, [hmIm][Tf_2N] and [pmIm][Tf_2N], the essentially identical temperature dependence of these properties in the supercooled liquid range illustrates the difficult of discerning the best theory only on the basis of linear behavior in plots $\ln(\eta)$ vs $1/(TS_{\text{exc}})$ or $\ln(\eta)$ vs $1/V_f$. Instead of discriminating which one is the correct theory, extensive calculations of configurational entropy of polymers showed the complementary information provided by theories based on S_c or V_f.[104] It has been shown that TS_c and V_f calculated for a given model of polymer follow proportionally each other within a large temperature range. The effective activation energy could be also related to other properties governing particle displacement, such as the high frequency shear modulus, G_∞,[41,85] and the mean-square displacement $\langle u^2\rangle$ that scales inversely with G_∞. Therefore, it should be also valid a relationship $TS_c \propto \langle u^2\rangle$.[104] All together, it is thus reasonable that the fast relaxation probed by I_{QES} exhibits the same temperature dependence as TS_{exc}, V_f, and $\langle u^2\rangle$ as shown in Fig. 8.

The detailed analysis of the structural relaxation of [hmIm][Tf_2N] in Ref. 11 allows for a further discussion of the $I_{\text{QES}}(T)$ curve of this system in a wide temperature range. The bottom panel in Fig. 7 shows $I_{\text{QES}}(T)$ for [hmIm][Tf_2N] within the 120–370 K range. The I_{QES} is essentially constant below T_g in the scale of Fig. 7, and the first change of slope takes place at a temperature compatible with the experimental T_g. The regime above T_g, but below $T \sim$ 260 K, can be fit by a linear relationship, whereas another linear regime starts with higher slope for temperatures above ~260 K, which is slightly below the melting temperature of [hmIm][Tf_2N], T_m = 270 K. Interestingly, the temperature of this second bending of the $I_{\text{QES}}(T)$ curve agrees with the temperature ~250 K at which a bifurcation between fast and slow modes has been observed in the investigation of structural relaxation of [hmIm][Tf_2N].[11] In terms of the mode coupling theory (MCT) of liquid dynamics,[105,106] for which the relaxation time decreases with temperature according to $\tau \propto (T - T_c)^{-\gamma}$, where γ and T_c are adjustable parameters, this characteristic temperature corresponds to the crossover temperature T_c. The MCT analyses of the OKE spectra of some ionic liquids suggested similar values, for instance, $T_c \sim$ 255 K for 1-ethyl-3-methylimidazolium nitrate,[107] $T_c \sim$ 231 K for *N*-propyl-3-methylpyridinium bis(trifluoromethylsulfonyl)imide,[108] and $T_c \sim$ 225 K for [bmIm][Tf_2N].[109] Therefore, we suggested that the second bending of the $I_{\text{QES}}(T)$ curves seen in Fig. 7 for [bmIm][Tf_2N] and [hmIm][Tf_2N] correspond to T_c (values given in Table I). Several investigations of fast dynamics in glass-forming liquids by low-frequency Raman spectroscopy indicated a signature of T_c as the temperature at which I_{QES} reaches a plateu and becomes temperature independent.[110–112] These analyses have been carried out mainly by using the coupling model for the relaxational and vibrational contributions of Raman spectra (not to be confused with the MCT theory for glass formation), in which I_{QES} is giving by the strength parameter $\delta^2(T)$ of coupling between relaxations and boson peak vibrations.[57–59,110–112] It is worth stressing that $\delta^2(T)$

becomes temperature independent at high temperature provided that the α-relaxation has been previously removed from the experimental data. This is not a straightforward procedure, and we are not performing here such a subtraction of the α-relaxation. Thus, I_{QES} does not probe only fast relaxation at high temperatures because slower relaxations now merge with the relaxation processes that result in the QES. Thus, the signature of T_c in Fig. 7 is another linear regime for $I_{QES}(T)$ above this temperature, rather than $I_{QES}(T)$ reaching a plateu at $T > T_c$.[110–112] Nevertheless, three characteristic temperatures, T_o, T_g, and T_c, can be discernible and distinct regimes of I_{QES} are probed by low-frequency Raman spectroscopy of the ionic liquid [hmIm][Tf_2N].

IV. CONCLUSIONS

Low-frequency Raman spectra unravel the intermolecular vibrations of ionic liquids in full agreement with results of OKE spectroscopy that has been used to study the short-time dynamics of these materials.[11,16,21–26] Even though the intermolecular vibrational dynamics is overlapped by the QES in low-frequency Raman spectra at high temperatures, the QES signal provides information on fast relaxations that are themselves interesting data for supercooled ionic liquids. Comparison of Raman spectra of ionic liquids with different cations corroborated the assignment of the spectral feature around 100 cm^{-1} as librational motion of the aromatic ring in imidazolium ionic liquids. The ionic liquids investigated in this work allowed discriminating fits with different number of bands in the low-frequency range. The boson peak is observed in low-frequency Raman spectra at temperatures close to T_g, as expected from the fragile characteristic of ionic liquids.[10–12,31,32] A correlation length $\xi \sim 19$ Å has been associated to the boson peak vibrations. Since the position of the boson peak and sound velocity[63–65,81] of ionic liquids are more dependent on anion than cation, the length ξ does not change with the length of the alkyl chain in 1-alkyl-3-methylimidazolium cations, in contrast to the position of the first-sharp diffraction peak observed in static structure factor of ionic liquids.[26,66–68] After normalizing the spectra by the high-frequency intramolecular bands of the common [Tf_2N] anion, we found that the low-frequency Raman spectra of ionic liquids based on imidazolium cations are significantly less intense than ionic liquids containing non-aromatic cations. This is expected because of the more polarizable moiety of the imidazolium ring, but an interestingly finding is that the relaxational and vibrational contributions change by the same amount among the aromatic and non-aromatic ionic liquids investigated in this work. This finding strongly supports the proposition that the fast relaxations and the boson peak vibrations are interrelated dynamics processes.[55–60,98–100,110–112] The ionic liquid [hmIm][TF_2N] is a particularly interesting system to investigate the QES intensity because it has been the subject of a detailed analysis of the structural relaxation in a wide temperature range.[11] It was first shown that previous data of structural relaxation[11] and excess entropy[87] are consistently interpreted on the basis of the Adam-Gibbs theory.[42,89–92] Furthermore, the size of the cooperatively rearranging regions calculated according to the AG theory is consistent with the correlation length ξ obtained from the boson peak vibrations. This finding supports the proposition that the same spatial scale is responsible for fast relaxations and vibrations unraveled by low-frequency Raman spectroscopy.[98–100] The temperature dependence of Raman spectra of [hmIm][TF_2N] allows one to distinguish in the $I_{QES}(T)$ the characteristic temperatures T_o, T_g, and T_c, as obtained from structural relaxation data.[11] The $I_{QES}(T)$ curve is similar to other properties such as excess entropy,[87] free volume,[96] and mean-square displacement,[97] illustrating correlations between fast and slow dynamics of glass-forming liquids. Although this work showed that structural relaxation of supercooled [hmIm][TF_2N] can be understood by the entropy based AG theory, the structural relaxation of [pmIm][TF_2N] has been interpreted instead by free volume based theories.[96] Recently, the simultaneous study of temperature and pressure effects allowed disentangling the role of thermal and density variations on the QES intensity of glass-forming liquids.[55] It has been shown that volume is more important above T_g, whereas thermal energy is more important below T_g.[55] Therefore, further works in our group will be dedicated to Raman spectroscopy studies of ionic liquids under pressure.

ACKNOWLEDGMENTS

The author is indebted to FAPESP and CNPq for financial support.

[1] T. Welton, Chem. Rev. **99**, 2071 (1999).
[2] P. Wasserscheid and T. Welton, *Ionic Liquids in Synthesis* (Wiley, New York, 2003).
[3] M. C. Buzzeo, R. G. Evans, and R. G. Compton, ChemPhysChem **8**, 1106 (2004).
[4] F. Karadas, M. Atilhan, and S. Aparicio, Energy Fuels **24**, 5817 (2010).
[5] M. Palacio and B. Bhushan, Tribol. Lett. **40**, 247 (2010).
[6] S. Werner, M. Haumann, and P Wasserscheid, Ann. Rev. Chem. Biomol. Eng. **1**, 203 (2010).
[7] C. P. Fredlake, J. M. Crosthwaite, D. G. Hert, S. N. V. K. Aki, and J. F. Brennecke, J. Chem. Eng. Data **49**, 954 (2004).
[8] A.-V. Mudring, Aust. J. Chem. **63**, 544 (2010).
[9] S. Aparicio, M. Atilhan, and F. Karadas, Ind. Eng. Chem. Res. **49**, 9580 (2010).
[10] W. Xu, E. I. Cooper, and C. A. Angell, J. Phys. Chem. B **107**, 6170 (2003).
[11] O. Russina, M. Beiner, C. Pappas, M. Russina, V. Arrighi, T. Unruh, C. L. Mullan, C. Hardacre, and A. Triolo, J. Phys. Chem. B **113**, 8469 (2009).
[12] C. Schreiner, S. Zugmann, R. Hartl, and H. J. Gores, J. Chem. Eng. Data **55**, 4372 (2010).
[13] C. A. Angell, Science **267**, 1924 (1995).
[14] C. A. Angell, K. L. Ngai, G. B. McKenna, P. F. McMillan, and S. W. Martin, J. Appl. Phys. **88**, 3113 (2000).
[15] H. Weingärtner, Angew. Chem., Int. Ed. **47**, 654 (2008).
[16] E. W. Castner, Jr. and J. F. Wishart, J. Chem. Phys. **132**, 12091 (2010).
[17] A. Rivera, A. Brodin, A. Pugachev, and E. A. Rossler, J. Chem. Phys. **126**, 114503 (2007).
[18] D. A. Turton, J. Hunger, A. Stoppa, G. Hefter, A. Thoman, M. Walther, R. Buchner, and K. Wynne, J. Am. Chem. Soc. **131**, 11140 (2009).
[19] M. Krüger, E. Bründermann, S. Funkner, H. Weingärtner, and M. Havenith, J. Chem. Phys. **132**, 101101 (2010).
[20] A. Triolo, O. Russina, C. Hardacre, M. Nieuwenhuyzen, M. A. Gonzalez, and H. Grimm, J. Phys. Chem. B **109**, 22061 (2005).
[21] B.-R. Hyun, S. V. Dzyuba, R. A. Bartsch, and E. L. Quitevis, J. Phys. Chem. A **106**, 7579 (2002).
[22] G. Giraud, C. M. Gordon, I. R. Dunkin, and K. Wynne, J. Chem. Phys. **119**, 464 (2003).
[23] J. Li, I. Wang, K. Fruchey, and M. D. Fayer, J. Phys. Chem. A **110**, 10384 (2006).

[24]H. Shirota, A. M. Funston, J. F. Wishart, and E. W. Castner, Jr., J. Chem. Phys. **122**, 184512 (2005).
[25]T. Fujisawa, K. Nishikawa, and H. Shirota, J. Chem. Phys. **131**, 244519 (2009).
[26]O. Russina, A. Triolo, L. Gontrani, R. Caminiti, D. Xiao, L. G. Hines,Jr., R. A. Bartsch, E. L. Quitevis, N. Pleckhova, and K. R. Seddon, J. Phys.: Condens. Matter **21**, 424121 (2009).
[27]S. Kojima, Phys. Rev. B **47**, 2924 (1993).
[28]H. Z. Cummings, G. Li, W. Du, R. M. Pick, and C. Dreyfus, Phys. Rev. E **53**, 896 (1996).
[29]S. N. Yannopoulos and G. N. Papatheodorou, Phys. Rev. B **62**, 3728 (2000).
[30]M. C. C. Ribeiro, L. F. C. de Oliveira, and N. S. Gonçalves, Phys. Rev. B **63**, 104303 (2001).
[31]M. C. C. Ribeiro, J. Phys. Chem. B **111**, 5008 (2007).
[32]M. C. C. Ribeiro, J. Chem. Phys. **132**, 024503 (2010).
[33]A. P. Sokolov, E. Rössler, A. Kisliuk, and D. Quitmann, Phys. Rev. Lett. **71**, 2062 (1993).
[34]A. P. Sokolov, A. Kisliuk, D. Quitmann, A. Kudlik, and E. Rössler, J. Non-Cryst. Solids **172–174**, 138 (1994).
[35]K. L. Ngai and M. Paluch, J. Chem. Phys. **120**, 857 (2004).
[36]Y. Umebayashi, T. Fujimori, T. Sukizaki, M. Asada, K. Fujii, R. Kanzaki, and S. Ishiguro, J. Phys. Chem. A **109**, 8976 (2005).
[37]R. W. Berg, Monatsch. Chem. **138**, 1045 (2007).
[38]T. Endo and K. Nishikawa, J. Phys. Chem. A **112**, 7543 (2008).
[39]M. J. Monteiro, F. F. C. Bazito, L. J. A. Siqueira, M. C. C. Ribeiro, and R. M. Torresi, J. Phys. Chem. B **112**, 2102 (2008).
[40]Q. Zhong and J. T. Fourkas, J. Phys. Chem. B **112**, 15529 (2008).
[41]J. C. Dyre, Rev. Mod. Phys. **78**, 953 (2006).
[42]G. Adam and J. H. Gibbs, J. Chem. Phys. **43**, 139 (1965).
[43]M. H. Cohen and D. Turnbull, J. Chem. Phys. **31**, 1164 (1959).
[44]D. Turnbull and M. H. Cohen, J. Chem. Phys. **34**, 120 (1961).
[45]L. Larini, A. Ottochian, C. de Michele, and D. Leporini, Nat. Phys. **4**, 42 (2008); A. Ottochian and D. Leporini, Philos. Mag. **91**, 1786 (2011).
[46]A. V. Blokhin, Y. U. Paulechka, A. A. Strechan, and G. J. Kabo, J. Phys. Chem. B **112**, 4357 (2008).
[47]M. Zanatta, G. Baldi, S. Caponi, A. Fontana, E. Gilioli, M. Krish, C. Masciovecchio, G. Monaco, L. Orsingher, F. Rossi, G. Ruocco, and R. Verbeni, Phys. Rev. B **81**, 212201 (2010).
[48]M. Cho, M. Du, N. F. Scherer, G. R. Fleming, and S. Mukamel, J. Chem. Phys. **99**, 2410 (1993); S. Kinoshita, Y. Kai, M. Yamaguchi, and T. Yagi, Phys. Rev. Lett. **75**, 148 (1995).
[49]R. Shuker and R. W. Gammon, Phys. Rev. Lett. **25**, 222 (1970).
[50]S. Y. Yannopoulos, K. S. Andrikopoulos, and G. Ruocco, J. Non-Cryst. Solids **352**, 4541 (2006).
[51]I. Pócsik and M. Koós, Solid State Commun. **74**, 1253 (1990).
[52]N. Shimodaira, K. Saito, N. Hiramitsu, S. Matsushita, and A. J. Ikushima, Phys. Rev. B **71**, 024209 (2005).
[53]J. A. Bucaro and T. A. Litovitz, J. Chem. Phys. **54**, 3846 (1971).
[54]M. L. P. Le, F. Alloin, P. Strobel, J.-C. Leprêtre, C. P. del Valle, and P. Judeinstein, J. Phys. Chem. B **114**, 894 (2010).
[55]L. Hong, B. Begen, A. Kisliuk, V. N. Novikov, and A. P. Sokolov, Phys. Rev. B **81**, 104207 (2010).
[56]G. Winterling, Phys. Rev. B **12**, 2432 (1975).
[57]V. Z. Gochiyaev, V. K. Malinovsky, V. N. Novikov, and A. P. Sokolov, Philos. Mag. **63**, 777 (1991).
[58]S. Kojima and V. N. Novikov, Phys. Rev. B **54**, 222 (1996).
[59]V. N. Novikov, A. P. Sokolov, B. Strube, N. V. Surovtsev, E. Duval, and A. Mermet, J. Chem. Phys. **107**, 1057 (1997).
[60]M. Krüger, M. Soltwisch, I. Petscherizin, and D. Quitmann, J. Chem. Phys. **96**, 7352 (1992).
[61]V. N. Novikov and A. P. Sokolov, Solid State Commun. **77**, 243 (1991).
[62]S. R. Elliott, Europhys. Lett. **19**, 201 (1992).
[63]C. Frez, G. J. Diebold, C. D. Tran, and S. Yu, J. Chem. Eng. Data **51**, 1250 (2006).
[64]R. G. de Azevedo, J. M. S. S. Esperança, J. Szydlowski, Z. P. Visak, P. F. Pires, H. J. R. Guedes, and L. P. N. Rebelo, J. Chem. Thermodyn. **37**, 888 (2005).
[65]M. Fukuda, M. Terazima, and Y. Kimura, J. Chem. Phys. **128**, 114508 (2008).
[66]A. Triolo, O. Russina, H.-J. Bleif, and E. di Cola, J. Phys. Chem. B **111**, 4641 (2007).
[67]A. Triolo, O. Russina, B. Fazio, G. B. Appetecchi, M. Carewska, and S. Passerini, J. Chem. Phys. **130**, 164521 (2009).
[68]C. Hardacre, J. D. Holbrey, C. L. Mullan, T. G. A. Youngs and D. T. Bowron, J. Chem. Phys. **133**, 074510 (2010).
[69]C. S. Santos, H. V. R. Annapureddy, N. S. Murthy, H. K. Kashyap, E. W. Castner, Jr., and C. J. Margulis, J. Chem. Phys. **134**, 064501 (2011).
[70]S. M. Urahata and M. C. C. Ribeiro, J. Chem. Phys. **120**, 1855 (2004).
[71]Y. Wang and G. A. Voth, J. Phys. Chem. B **110**, 18601 (2006).
[72]J. N. A. C. Lopes and A. A. H. Pádua, J. Phys. Chem. B **110**, 3330 (2006).
[73]K. Shimizu, M. F. C. Gomes, A. A. H. Pádua, L. P. N. Rebelo, and J. N. C. Lopes, J. Mol. Struct.: THEOCHEM **946**, 70 (2010).
[74]S. L. Chan and S. R. Elliott, Phys. Rev. B **43**, 4423 (1991).
[75]D. Morineau and C. Alba-Simionesco, J. Chem. Phys. **109**, 8494 (1998).
[76]M. A. Marques, M. I. Cabaço, M. I. B. Marques, and A. M. Gaspar, J. Phys.: Condens. Matter **14**, 7427 (2002).
[77]M. C. C. Ribeiro, J. Phys.: Condens. Matter **17**, 453 (2005).
[78]M. Wilson and P. A. Madden, Phys. Rev. Lett. **80**, 532 (1998).
[79]C. Massobrio and A. Pasquarello, J. Chem. Phys. **114**, 7976 (2001).
[80]L. Börjesson, A. K. Hassan, J. Swenson, and L. M. Torell, Phys. Rev. Lett. **70**, 1275 (1993).
[81]R. G. de Azevedo, J. M. S. S. Esperança, V. Najdanovic-Visak, Z. P. Visak, H. J. R. Guedes, M. N. da Ponte, and L. P. N. Rebelo, J. Chem. Eng. Data **50**, 997 (2005).
[82]T. Scopigno, G. Ruocco, F. Sette, and G. Monaco, Science **302**, 849 (2003).
[83]M. C. C. Ribeiro, T. Scopigno, and G. Ruocco, J. Chem. Phys. **128**, 191104 (2008).
[84]U. Buchenau and R. Zorn, Europhys. Lett. **18**, 523 (1992).
[85]V. N. Novikov, Y. Ding, and A. P. Sokolov, Phys. Rev. E **71**, 061501 (2005).
[86]A. V. Blokhin, Y. U. Paulechka, and G. J. Kabo, J. Chem. Eng. Data **51**, 1377 (2006).
[87]Y. Shimizu, Y. Ohte, Y. Yamamura, K. Saito, and T. Atake, J. Phys. Chem. B **110**, 13970 (2006).
[88]J. Salminen, N. Papaiconomou, R. A. Kumar, J.-M. Lee, J. Kerr, J. Newman, and J. M. Prausnitz, Fluid Phase Equilib. **261**, 421 (2007).
[89]R. Richert and C. A. Angell, J. Chem. Phys. **108**, 9016 (1998).
[90]G. P. Johari, J. Chem. Phys. **112**, 8958 (2000).
[91]M. Goldstein, J. Chem. Phys. **123**, 244511 (2005).
[92]J. C. Dyre, T. Hechsher, and K. Niss, J. Non-Cryst. Solids **355**, 624 (2009).
[93]T. Kanaya, T. Tsukushi, K. Kaji, J. Bartos, and J. Kristiak, Phys. Rev. E **60**, 1906 (1999).
[94]A. M. Funston, T. A. Fadeeva, J. F. Wishart, and E. W. Castner, Jr., J. Phys. Chem. B **111**, 4963 (2007).
[95]H. Tokuda, K. Hayamizu, K. Ishii, Md. A. B. H. Susan, and M. Watanabe, J. Phys. Chem. B **109**, 6103 (2005).
[96]G. Dlubek, Y. Yu, R. Krause-Rehberg, W. Beichel, S. Bulut, N. Pogodina, I. Krossing, and Ch. Friedrich, J. Chem. Phys. **133**, 124501 (2010).
[97]O. Yamamuro, Y. Inamura, S. Hayashi, and H. Hamaguchi, Flow Dynamics **832**, 73 (2006).
[98]D. Quitmann, M. Soltwisch, and G. Ruocco, J. Non-Cryst. Solids **203**, 12 (1996).
[99]D. Quitmann and M. Soltwisch, Philos. Mag. B **77**, 287 (1998).
[100]D. Quitmann and M. Soltwisch, J. Non-Cryst. Solids **235–237**, 237 (1998).
[101]K. Niss, C. Dalle-Ferrier, B. Frick, D. Russo, J. Dyre, and C. Alba-Simionesco, Phys. Rev. E **82**, 021508 (2010).
[102]W. Kauzmann, Chem. Rev. **43**, 219 (1948).
[103]G.-E. Logotheti, J. Ramos, and I. G. Economou, J. Phys. Chem. B **113**, 7211 (2009).
[104]J. Dudowicz, K. F. Freed, and J. F. Douglas, Adv. Chem. Phys. **137**, 125 (2008).
[105]W. Götze and L. Sjögren, Rep. Prog. Phys. **55**, 241 (1992).
[106]S. Das, Rev. Mod. Phys. **76**, 785 (2004).
[107]H. Cang, J. Li, and M. D. Fayer, J. Chem. Phys. **119**, 13017 (2003).
[108]J. Li, I. Wang, K. Fruchey, and M. D. Fayer, J. Phys. Chem. A **110**, 10384 (2006)
[109]B. G. Nicolau, A. Sturlaugson, K. Fruchey, M. C. C. Ribeiro, and M. D. Fayer, J. Phys. Chem. B **114**, 8350 (2010).
[110]N. V. Surovtsev, A. M. Pugachev, B. G. Nenashev, and V. K. Malinovsky, J. Phys.: Condens. Matter **15**, 7651 (2003).
[111]N. V. Surovtsev, J. Phys.: Condens. Matter **19**, 196101 (2007).
[112]I. V. Prots, V. K. Malinovsky, and N. V. Surovtsev, Glass Phys. Chem. **34**, 30 (2008).